



Characterizing heat release rate transients

Rodney Bryant*, Erik Johnsson, George Mulholland¹

Fire Research Division, National Institute of Standards and Technology, Gaithersburg, MD 20899, USA

ARTICLE INFO

Article history:

Received 2 August 2011

Received in revised form

1 March 2012

Accepted 4 April 2012

Keywords:

Heat release rate

Fire growth

Fire hazard evaluation

Measurement response time

Calorimetry

ABSTRACT

A series of experiments was performed to characterize the time response of a large-scale open calorimeter to square-wave pulses in terms of peak heat release rate, width of the peak, and conservation of energy. Quantitative heat release rate measurements of full-scale fires up to 2.7 MW were conducted using the principle of oxygen-consumption calorimetry. A remotely-operated natural gas burner provided a reproducible heat source and near-square-wave inputs to the system. The calorimeter was capable of resolving the actual peak heat release rate value for fire transient events having a full width at half height of 15 s or greater. However, if the full width at half height measured by the calorimeter was less than 11 s, the measured peak value underestimated the actual peak heat release rate by 15% or more. Even if the peak heat release rate could not be fully resolved, the calorimeter was able to provide an estimate of the total heat released to within about 5%, demonstrating conservation of energy by the system.

Published by Elsevier Ltd.

1. Introduction

Heat release rate (HRR) measurements provide information essential to defining the fire safety characteristics of products and for determining the magnitudes of fires involving multiple products in research structures. The heat release rate of a burning item or combination of items directly impacts the temperatures of the surroundings, fire spread, and the generation of toxic gases. Thus, it is important that the HRR measurement be made in a quantitative manner with an understanding of the limitations of the measurement. The most commonly used method of measuring HRR is oxygen-consumption calorimetry which uses a combination of measurements from the exhaust flue to compute HRR.

Peak HRR is often relied upon for determining the potential for spread of hazardous conditions. For this reason, fire safety and product flammability testing regulations are frequently based on maximum allowed rates of heat release. Therefore, it is important that not just steady HRRs are measured accurately, but that the transient HRRs of fires are measured as well. Different calorimeter facilities have differing time responses and thus differing tendencies to smooth out a brief peak. Some facilities use an open hood while others use a compartment which allows smoke to build up prior to spilling into the hood, thus adding a delay in the measurement of heat release rate.

* Corresponding author. Tel.: +1 301 975 6487.

E-mail address: rodney.bryant@nist.gov (R. Bryant).

¹ Present address: Department of Mechanical Engineering, University of Maryland, College Park, MD 20742, USA.

Messerschmidt and van Hees [1] discussed this transient response issue in the context of the European Community's Single Burning Item Test, which is based on a heat release rate measurement. It is shown that different laboratories could end up rating a product differently in this test solely as a result of the differing transient behavior characteristics of their measurement systems. They recommend that the oxygen meter's apparent response time fall within a window of 9–12 s, in order to minimize the tendency of separate laboratories to rate a product differently in the Single Burning Item test.

Another aspect of transient system response is related to noise in the calculated heat release rate. System noise (a result of the random variations in all of the variables entering into the heat release rate calculation) can affect the apparent magnitude of a heat release peak, and thus its uncertainty. The effect depends on the root mean square noise level and its frequency characteristics relative to the peak duration. An approach that is sometimes used is to judge a tested product's performance on the basis of a heat release rate curve subjected to a running time-averaging process. The longer the time interval used for averaging, the more the noise is filtered out but also the real and rapid heat release rate changes are damped. This raises the question: What duration of a heat release rate fluctuation matters when an object is burning in some context such as a compartment fire? Because of the dampening effects of data smoothing, the smoothing interval should be reported along with the heat release rate data if applied. Sette [2] evaluated the post-processing of the data with running averages and other filtering techniques. Instead of applying a running average to the data, he recommends applying some of the filtering features of the instrumentation along with post

process filtering to improve the temporal resolution of the system.

The present study describes a series of experiments performed to characterize the time response of a large-scale open calorimeter. Transient events of HRR were generated using a natural gas burner. The resulting response of the calorimeter was evaluated with respect to peak HRR, width of the peak, and the conservation of energy. The study demonstrates a method to determine the real response time of a similar measurement system and ultimately its ability to resolve transient events.

2. Description of experiments

The large-scale open calorimeter in the NIST Large Fire Research Facility measures HRR by the principle of oxygen-consumption calorimetry. The resulting HRR value is computed from a combination of measurements made in the exhaust flue, Eq. (1). The HRR equation is described in detail in Refs. [3,4].

$$\text{HRR}_{\text{calorimeter}} = \left[(\Delta H_c)_{\text{Mass}_O_2}^{\text{HC}} \phi - ((\Delta H_c)_{\text{Mass}_O_2}^{\text{CO}} - (\Delta H_c)_{\text{Mass}_O_2}^{\text{HC}}) \frac{1 - \phi X_{\text{CO}}}{2 X_{O_2}} \right] \times \frac{\dot{m}_e}{1 + \phi(\alpha - 1)} (1 - X_{H_2O}^o) X_{O_2}^o \frac{M_{O_2}}{M_{\text{air}}} \quad (1)$$

where $(\Delta H_c)_{\text{Mass}_O_2}^{\text{HC}}$ is the heat of combustion of hydrocarbon fuel per mass of oxygen consumed (MJ/kg O_2), and $(\Delta H_c)_{\text{Mass}_O_2}^{\text{CO}}$ is the heat of combustion of carbon monoxide per mass of oxygen consumed (MJ/kg O_2),

$$\phi = \frac{X_{O_2}^o (1 - X_{CO_2} - X_{CO}) - X_{O_2} (1 - X_{CO_2}^o)}{(1 - X_{O_2} - X_{CO_2} - X_{CO}) X_{O_2}^o} = \text{oxygen depletion factor,}$$

where \dot{m}_e is the mass flow rate in the exhaust duct (kg/s), α is the combustion products expansion factor, M_i is the molecular weight of gas i (kg/kmol), X_i is the volume fraction of exhaust gas i and X_i^o is the volume fraction ambient gas i .

The facility also contains a natural gas burner with electronic flow control. The burner provides an accurate input of HRR as well as an independent confirmation of the calorimetry measurement. A data acquisition system samples each measurement at a rate of 200 Hz, and electronically averages the signals over a period of 1 s before they are stored to a computer. A detailed description of the physical characteristics—the calorimeter, burner, and data acquisition system, is presented in Ref. [3]. The sections that follow provide a description of the temporal characteristics of the systems that are important to the scope of this study as well as the procedures used to conduct the experiments.

2.1. Natural gas burner

The natural gas burner, shown in Fig. 1, can produce flows that correspond to a wide range of heat release rates, from 50 kW to over 6 MW in any increments specified by the user. The heat release rate of the burner is computed from the heating value of the natural gas, $(\Delta H_c)_{\text{NG}}$, and the measured flow of natural gas, \dot{V} , corrected for temperature, T , and pressure, P , Eq. (2). The volumetric gas flow meter is a rotary device which displaces a fixed volume of gas four times per revolution. The device produces digital pulses at a rate of about 1 pulse per 2 L of gas. A heat release rate of 1.0 MW corresponds to about 7 pulses/s and 2.5 MW to about 18 pulses/s.

$$\text{HRR}_{\text{burner}} = \dot{V} \frac{P}{P_{\text{ref}}} \frac{T_{\text{ref}}}{T} (\Delta H_c)_{\text{NG}} \quad (2)$$

The pulse counting allows an accurate estimate of the average heat release rate for longer periods but the relatively low number of pulses per second at the smaller HRR values limited the



Fig. 1. Photo of a 3 MW fire from the natural gas burner.

resolution needed for the study of transient events. To provide a more rapid response to the transient events over the full range of HRR, a Schmidt–Boelter type radiometer with a time constant of 0.1–0.2 s was used. The radiometer was set up at a distance of 4 m from the burner with a view that included the entire flame volume.

2.2. Calorimeter

The large-scale calorimeter is an open system that collects the products of the fire and the surrounding ambient air in an exhaust hood above the fire. Measurements of the flow of gas through the hood and gas composition are performed to determine the amount of oxygen consumed by the fire. Gas species measurements include oxygen, carbon dioxide (CO_2), and carbon monoxide (CO). The oxygen analyzer is a paramagnetic device that takes advantage of the strong magnetic susceptibility of oxygen molecules, and the CO_2 and CO analyzers are both non-dispersive infrared absorption devices. Each instrument contributes to the overall response time of the system. Initially, there will not be a response since the information about the change has to reach the instruments. The first component of response to a transient event is the gas travel time from the flame tips to the location in the duct where the gases are sampled; this time varies with the hood flow rate. Next, there is the gas travel time from the gas sample location to the inlet of the instruments. This time is independent of hood flow rate but depends on the sample flow rate and size of the plumbing. Finally, there is the response time of the instruments. This time is fixed when the flow rate to each instrument is set at its manufacturer-recommended value.

In general one needs to measure the lag time (total sample flow time) from the fire to the instrument inlet. This may have a different value for each instrument which is determined by flow path and flow rate to the instrument. Lag time is used to synchronize the measurements that go into the heat release rate calculation. One also needs to measure and take note of the system response times for the individual gas measuring

instruments. These are to be kept within a certain range since they affect how closely the system will follow a given time-varying heat release rate process from the fire being measured. In particular, system response times affect accurate measurement of brief heat release rate peaks.

Precise values of the lag time for each instrument are needed since they must be incorporated into the data handling that results in a correct calculation of heat release rate. Measurement of these times was facilitated by abruptly changing the magnitude of the heat source—the natural gas burner. This capability was achieved via a flow control valve that was actuated on commands from a computer.

The first time interval, the flow delay to reach the gas sampling plane in the duct, was determined by calculating the difference between the time when the natural gas flow increased and the time at which any thermocouple near the sampling plane began to register a gas temperature increase of 3 K [1]. This time interval will vary with the hood flow rate, but was typically in the range of 4–8 s.

The second component of the lag time for a given instrument, the time to flow from the gas sample plane to the inlet of the instrument, is determined by the sample flow rate and the length of the flow path to each instrument. Fig. 2 is a diagram of the gas sample flow path. The gas sample is taken from the exhaust duct through a heated tube; it is then cooled and dried using a dry ice trap and desiccant; and then it is passed to the gas analyzers. The time can vary for different instruments because the flow paths differ. This component of the lag time was found by noting the

time between the thermocouple response and the instrument response to the fire-altered gases.

Ref. [1] recommends taking the time when the oxygen meter reading shows a change of 0.05% and the CO₂ meter a change of 0.02%. The estimated standard uncertainty of the oxygen and carbon dioxide measurements was $\pm 0.05\%$ O₂ and $\pm 0.03\%$ CO₂, respectively. This is of the same order as the recommended change criteria. The response of both instruments is linear with respect to gas concentration. Therefore, determining the transient times and response times can be accomplished by analyzing the changes in the instrument outputs, not the absolute scaled value of the output. A noisy output voltage would have greater impact on evaluating the change than the absolute accuracy of the instruments. Since the noise of the steady state response of the instruments was less than 50% of the recommended change criteria, these criteria were adopted for this study. The natural gas burner did not produce detectable levels of CO. The lag time component for the CO meter was assumed to be the same as for the CO₂ meter since they were effectively in the same flow system. The flow times between the sampling plane and instruments were on the order of a few seconds.

System response time is defined in Ref. [1] as the time required for the oxygen meter to go from 10% to 90% of the change induced by a step change in fire size. The response time of the system is limited by the instrument with the longest response time which tends to be the oxygen meter rather than the CO or CO₂ meters. Along the entire path, the gas does not travel as a rigid slug; rather it tends to undergo mixing with gases

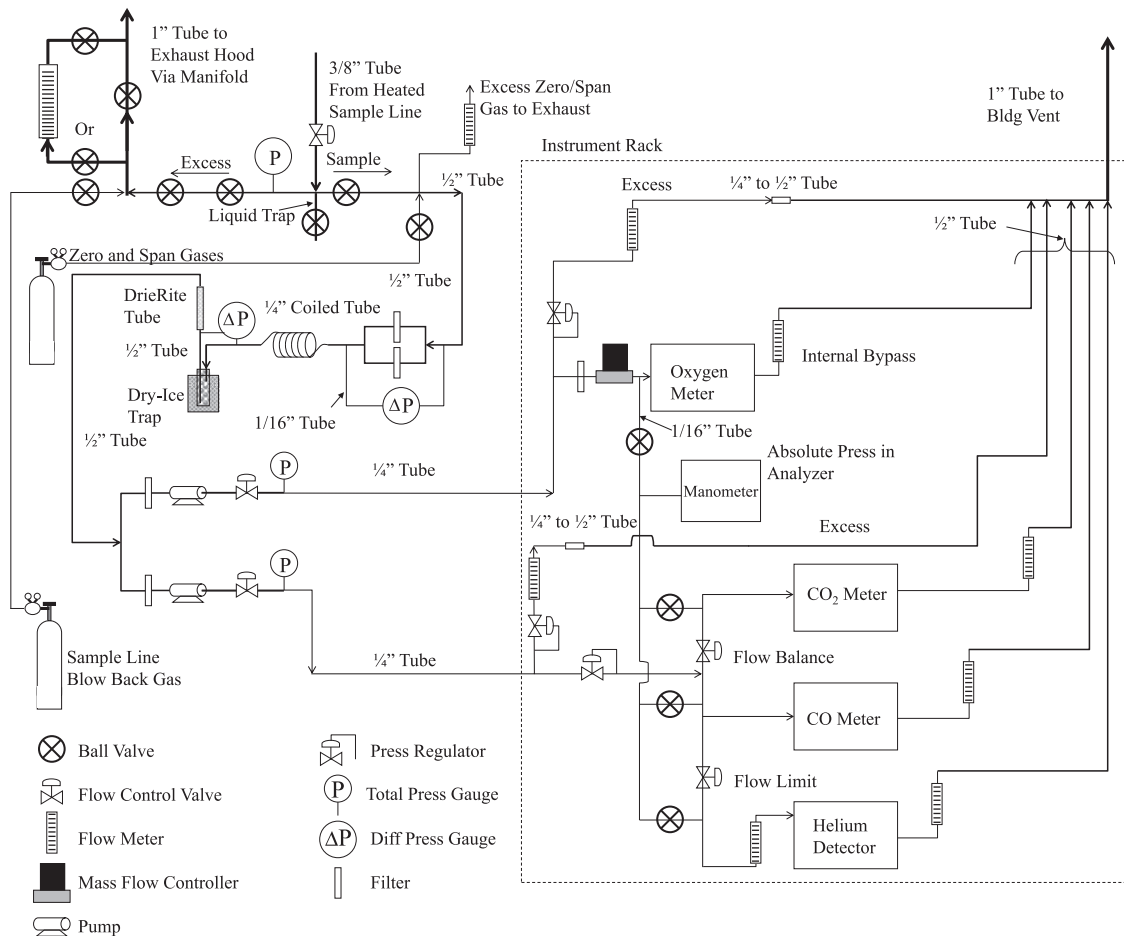


Fig. 2. Diagram of the gas analysis flow path.

originating earlier or later as a result of various turbulent mixing processes. This process, called dispersion, also affects the time response of the overall system to a change in the fire behavior. Careful design helps to minimize this effect. Any and all dispersion in the system, from the fire plume tip all the way to the gas analysis instrument, contributes to the time it takes for this signal to change from 10% to 90%. This dispersion smears the original time sequence of events in the fire. In particular, it decreases the reading of any heat release rate peak that occurs on a time scale comparable to or shorter than this 10–90% response time of the system.

The total system delays were somewhat longer than the sum of the constituent delays. For example, the total delay was 25 s for a particular experiment where, as a first approximation, the duct flow time (fire to sampling point at $9.9 \text{ m}^3/\text{s}$) $\approx 7 \text{ s}$, the gas sample flow time from the exhaust duct sample plane to the gas analysis system $\approx 2\text{--}3 \text{ s}$, and the instrument response times at nominal flow rates $\approx 5\text{--}10 \text{ s}$. The longer measured delay is likely due to the time required for the sample to pass through the humidity removal section of the gas analysis system.

2.3. Experimental procedures

The basic approach to assess system time response was to provide a square-wave pulse of heat release rate using the natural gas burner to simulate a transient fire event such as a peak in HRR. The amplitude of the pulse or peak HRR was set at nominal values of 0.5 MW, 1.0 MW, and 2.5 MW using a flow control valve. The measurement sequence began by setting the burner at a heat release rate of 0.10 MW. This pilot level of heating was needed to efficiently ignite the rapidly increasing gas flow. The mass flow controller was set for a flow corresponding to 0.5 MW heat release rate and then a switch was activated which in turn opened the mass flow controller valve. After a fixed time, the sequence was reversed and the heat release set back to the pilot level, 0.1 MW. After the calorimeter reached a steady heat release at the pilot level, a repeat run would be made following the same procedure as above. Typically three runs were made for each of four pulse times: 30 s, 15 s, 10 s, and 5 s. At least one measurement was also made for a 60 s pulse. This sequence was then repeated for heat release rates of 1.0 MW and 2.5 MW.

To provide a more rapid response to the actual heat release of the burner, the output of the radiometer was used in conjunction with the burner measurement. The corrected burner peak heat release was obtained by multiplying the radiometer output with a calibration factor determined for each of the three heat release rates. To determine this calibration factor, the heat release rate computed from the natural gas burner volume flow measurement and radiometer output were averaged over a 20 s period during the steady burning for each of the three heat release rates. The calibration factor was computed as the ratio of the average heat release rate to the average radiometer voltage. The ratios have a dependence on fire size with values decreasing by 30% for a five-fold increase in the heat release rate (2.62 GW/V at 0.5 MW, 2.20 GW/V at 1 MW, and 1.85 GW/V at 2.5 MW).

3. Results and discussion

In principle this is a problem which can be treated as a deconvolution of the actual heat release rate versus time from the measured heat release and the system response characteristics [5,6]. Thus one solves an integral equation relating observed heat release rate to the time integral of actual heat release rate modulated by the measurement system response. Different mathematical techniques have been demonstrated in the noted

references. The inferred correction to the apparent heat release rate history is sometimes large ($O(100\%)$), particularly for cases in which the heat release rate peak width is comparable to the time response of the measurement system. However, the deconvolution process is quite sensitive to noise in the data and to the errors in the system response function [7]. Since it is unclear where both of these issues are significant, this study focuses on characterizing the time response for the domain in which the open calorimeter system gives accurate results. It should be noted that the combined measurements of the flow of the natural gas burner, the radiant energy from the fire, and the heat release rate (calorimetry) create the capability for future studies to assess the accuracy of various deconvolution algorithms.

The shape of the pulses for the burner HRR and the flame radiation (radiometer) are qualitatively similar as shown in Fig. 3. The limited signal resolution of the flow meter is apparent from the discrete change in heat release rate at the rise and fall of the pulse. There was a 1–2 s delay in the processing of the pulse counting relative to the radiometer measurement. This delay was observed in all the tests and has been removed for clarity from all figures where both traces are displayed. The radiometer provides a better representation of the heat release pulse shape since it responds to the flame intensity, and it has a faster response time than the gas flow meter. The inflection point of the radiometer output near the end of the pulse is thought to result from continued flow through the burner after the valve for the flow controller had been reset to the baseline level. The gas continues to drain as pressure in the gas line to the burner equilibrates to the lower baseline level.

Fig. 4 illustrates the characteristics of the square-wave pulse shapes for the 1 MW fire for the four different pulse widths. The 25 s time delay for the calorimeter was a result of the gas sampling time together with the nominal 9 s response time of the oxygen analyzer. For the 30 s and 15 s pulses, the peak in the calorimeter output is close to that of the burner and the full widths at the half height (FWHH) are similar though the curve shape produced by the calorimeter is rounded rather than square. The calorimeter peak is slightly reduced for the 10 s pulse and is reduced by about a factor of two for the 5 s pulse. In these two cases the FWHH values are also increased relative to the radiometer output. The pulse experiments for the remaining heat release rates provided similar results.

For 15 s square-wave pulses, Fig. 5 demonstrates that the peak heights are similar to those of the natural gas burner, the FWHH are similar to those from the radiometer, and that the shapes of all three calorimeter-generated curves are similar. There are slight differences in the radiometer-generated pulse shapes such as a flatter top section and a more abrupt decrease in the HRR at the end of the pulse for the larger heat release rates. These subtle

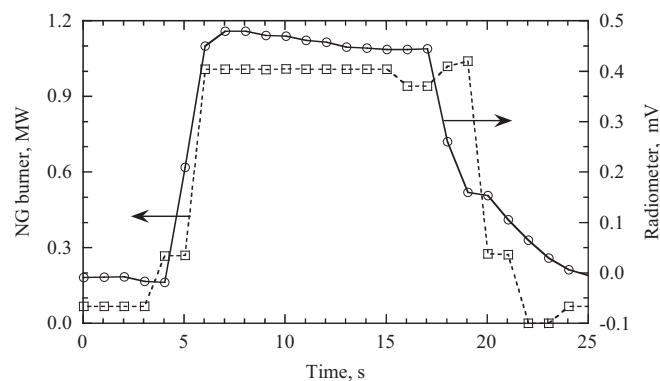


Fig. 3. The square-wave pulse measured by the radiometer and the burner flow meter for a 15 s release of natural gas for a 1 MW heat release rate.

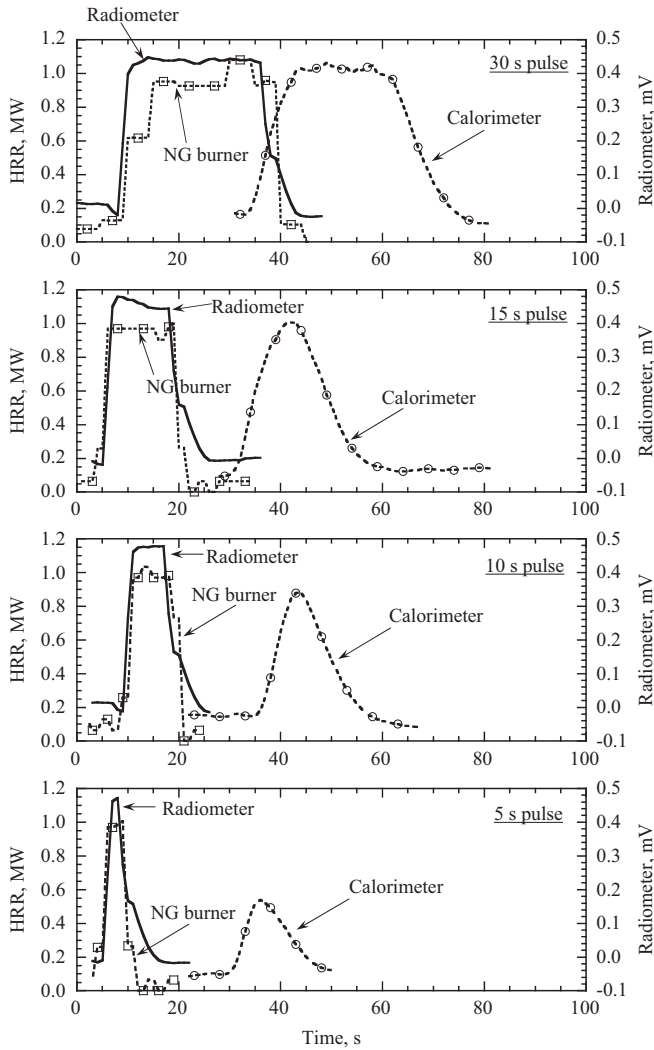


Fig. 4. The measured output versus time for the natural gas (NG) burner (□, left axis), calorimeter (○, left axis), and radiometer (solid line, right axis) resulting from 1 MW square-wave pulses of 30 s, 15 s, 10 s, and 5 s.

changes do not seem to be reflected in the calorimeter-generated curves.

If the gas burner is operating at 100% efficiency and the calorimeter is operating ideally, the gas burner heat release rate should be equal to the value determined based on oxygen consumption by the calorimeter. Both conditions were assumed to be true and therefore total heat release rate, the area under the HRR trace, for the calorimeter and the burner should be equivalent. A quantitative assessment of energy conservation was made by integrating the area under the curves to determine the total heat released from the burner flow measurement and from the calorimeter measurement. The total heat released for the pulse was defined as that above the baseline. The baseline correction was estimated as the average of the baseline values before and after the pulse. The ratios for the integrated calorimeter output to the integrated output of the burner are listed in Table 1. The average calorimeter to burner ratio for total heat released was 0.98 ± 0.05 and ranged from 0.89 to 1.06. The largest deviation from 1.0 occurred for the 5 s pulse at 1 MW. It is thought that the low number of pulses, about 3, counted per second was responsible for this deviation.

Taking advantage of the more rapid response time of the radiometer, a corrected total burner heat release was obtained by integrating the radiometer output and then multiplying it by a

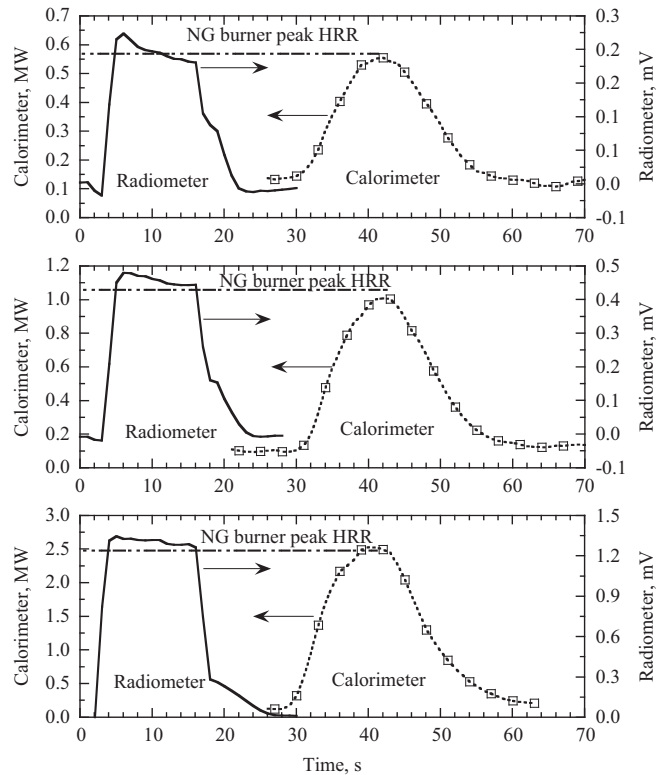


Fig. 5. The HRR measured by the calorimeter and the radiometer output for 15 s pulses of HRR inputs of 0.5 MW, 1.0 MW, and 2.5 MW. The measured peak from the natural gas burner is displayed as a dashed line.

calibration factor. The calibration factor was selected so that the total radiometer “energy” equaled the total heat released from the gas burner for the 30 s experiments. The ratios of calorimeter to radiometer total heat release are also listed in Table 1. The average calorimeter to radiometer ratio for total heat released around unity, therefore demonstrating that energy conservation had been established. There was an increased uncertainty for the shortest pulse length. For the 5 s pulses, the range in the standard deviation was 4–7% of the mean compared to a more typical range of 1–4% of the mean for the longer pulses.

A summary of the average peak HRR and FWHH and the associated standard deviations are given in Tables 2 and 3 for each set of three or more repeat measurements. The FWHH was computed based on the half-height above the baseline value. The peak HRR was not adjusted for the baseline value. For pulse lengths of 15 s and longer, the calorimeter peak was within 9% of the burner peak. The peaks corresponded to the instantaneous maximum values recorded by the calorimeter, the corrected burner, or the radiometer. The results indicate that the calorimeter peak is about 15% smaller than the burner peak for the 10 s pulse and about 50% smaller for the 5 s pulse. The results in Table 2 indicate that the calorimeter peak value was on average equivalent to the burner peak (average ratio = 1.03 ± 0.04) for square-wave pulses having widths equal to or greater than 15 s. However, the calorimeter significantly underestimated the peak height for square wave pulses lasting less than 10 s.

The FWHH time based on the calorimeter for the 1 MW fire was at most 10% longer than the radiometer time for the 15 s and 30 s pulse experiments while it is about 25% longer for the 10 s pulse and more than a factor of two longer for the 5 s pulse. Another observation is that the FWHH measured by the calorimeter remained relatively constant as the pulse width was

Table 1
Energy conservation results.

Nominal pulse width (s)	Integrated calorimeter output/Integrated burner output	Integrated calorimeter output/Integrated radiometer output
0.5 MW		
30	0.97 ± 0.01	0.97 ± 0.04
15	1.01 ± 0.03	0.98 ± 0.02
10	0.96 ± 0.01	0.92 ± 0.03
5	0.90 ± 0.06	0.92 ± 0.04
1.0 MW		
30	1.06 ± 0.02	1.06 ± 0.02
15	0.96 ± 0.03	1.05 ± 0.03
10	0.98 ± 0.02	1.10 ± 0.02
5	0.89 ± 0.04	1.05 ± 0.06
2.5 MW		
30	1.02 ± 0.01	1.02 ± 0.01
15	1.02 ± 0.02	1.05 ± 0.01
10	1.02 ± 0.02	1.07 ± 0.01
5	0.97 ± 0.04	1.06 ± 0.07

Table 2
Square-wave pulse results for peak HRR and FWHH.

Pulse width (s)	Calorimeter peak/Burner peak	Radiometer FWHH (s)	Calorimeter FWHH (s)
0.5 MW			
60 ^a	1.03	59	58
30	0.97 ± 0.02	28.0 ± 0.2	29.3 ± 0.3
15	1.01 ± 0.06	12.6 ± 0.1	14.4 ± 0.2
10	0.89 ± 0.05	8.7 ± 0.6	11.1 ± 0.4
5	0.58 ± 0.02	3.8 ± 0.6	8.9 ± 0.7
1.0 MW			
60	1.06 ± 0.03	58.6 ± 0.7	59.3 ± 0.8
30	1.06 ± 0.01	29.3 ± 1.2	30.0 ± 1.7
15	0.96 ± 0.01	13.8 ± 0.5	15.2 ± 0.7
10	0.82 ± 0.06	8.1 ± 0.5	10.8 ± 0.3
5	0.52 ± 0.03	3.4 ± 0.2	8.9 ± 0.3
2.5 MW			
60 ^a	1.09	58	58
30	1.05 ± 0.03	28.2 ± 0.9	28.2 ± 0.8
15	1.04 ± 0.02	14.4 ± 0.1	14.7 ± 0.2
10	0.88 ± 0.03	8.7 ± 0.8	10.6 ± 0.1
5	0.47 ± 0.02	3.4 ± 0.2	10.3 ± 0.4

^a Only one test performed.

Table 3
Square-wave pulse coefficient of variation.

Nom. pulse width (s)	Corrected burner peak (MW)	Burner CV	Calorimeter peak (MW)	Calorimeter CV
0.5 MW				
30	0.59	0.01	0.56	0.02
15	0.56	0.04	0.56	0.03
10	0.56	0.05	0.45	0.02
5	0.54	0.04	0.34	0.10
Avg ± σ	0.56 ± 0.02			
1.0 MW				
30	1.00	0.02	1.06	0.02
15	1.05	0.01	1.00	0.01
10	1.05	0.03	0.85	0.06
5	1.04	0.01	0.53	0.04
Avg ± σ	1.04 ± 0.02			
2.5 MW				
30	2.53	0.02	2.63	0.02
15	2.47	0.01	2.57	0.01
10	2.52	0.01	2.23	0.04
5	2.46	0.02	1.14	0.02
Avg ± σ	2.50 ± 0.04			

reduced from 10 s to 5 s. In this limit, the calorimeter response was controlled by the time response of the oxygen analyzer so that the response time approached a constant independent of the length of the square-wave pulse.

The response of the calorimeter to the square-wave pulses suggests a possible method for checking whether the peak heat release rate is changing too rapidly to obtain an accurate heat release rate with the calorimeter. If the FWHH is 15 s or longer for the HRR calorimeter, then one has confidence from this study that the heat release is accurately represented by the data. However, if the FWHH is less than 11 s the peak heat release will likely be underestimated by 15% or more. It does not appear to be possible to correct the peak heat release rate based on the FWHH, since small changes in the FWHH can result in a factor of two or more increase in the peak heat release rate, as seen in the data in Table 2. On the other hand, the square-wave pulse data may be useful in testing algorithms such as that developed by Abramowitz and Lyon for deconvoluting the actual heat release rate from the measured values.

As noted previously, the rise time of the oxygen, CO₂ and CO signals depends not only on the inherent instrument response time but also on the timewise dispersion of the gas concentration gradient due to mixing in the plume capture and gas sampling systems. Thus, the overall system response time assessed in the previous section is a product of various dispersion processes as well as instrument response characteristics. The dominant response time in the gas sample analysis system is that due to the oxygen analyzer, which has a nominal response time of 8 s. In the absence of a room as a container for the fire being measured and also in the absence of significant smoke back-up in the hood, it was estimated that the dispersive elements in the system will add roughly 5 s to the response time. The result is an overall response time of about 12–13 s (ignoring flow lag times) which is in reasonable agreement with the results of the experiments presented. It should be noted that use of a room or the existence of smoke back-up in the hood will increase the response time significantly.

A second important issue is the effect of the random system noise on the apparent magnitude of the heat release peak and thus the uncertainty in the peak height. The random noise sources include the gas analyzers, the pressure transducers for measuring velocity, the thermocouples, real variations in the temperature, velocity, and gas levels being measured, variations in the pumps and exhaust fans, and changing ambient humidity and temperature. By looking at the peak heat release rate in repeat tests under nominally identical conditions, the effect of the calorimeter-related

noise sources on the measured peak can be assessed. A convenient measure of repeatability is the coefficient of variation (CV), which is defined as the ratio of the standard deviation for repeat measurements to the average value. The results presented in Table 3 show that the CV for corrected peak burner heat release rate was at most 0.05 for any of the 12 sets of tests with at least three repeats. The CV was 0.02 or less for 5 of the 6 sets of tests with pulse widths of 15 s or 30 s. The CV for the calorimeter was also found to be in the range of 0.01–0.02 for 5 of the 6 sets of tests with pulse widths of 15 s or 30 s. The near equality of the CV's suggests that the calorimetry repeatability may be limited by the slight lack of repeatability in the square-wave pulse produced by the burner. Larger CVs up to 0.10 are obtained for heat release rate by the calorimeter for the 5 s and 10 s square-wave pulses.

It is encouraging that the contribution of the system noise to the CV for the peak heat release rate for the 30 s and 15 s square-wave pulses is typically 0.01–0.02. However, this does not mean that the CV for repeat burns of identical furnishing items, consumer products, or building materials will be as small. The CV in HRR measurements for such materials may be far greater than 0.02 because the identical items may not really be "identical" due to material and/or construction variation or because the flame spread process occurring on real objects is very sensitive to the details of the ignition process as well as the ambient flow and temperature field. Fire growth processes on real objects of any complexity (e.g., mattresses or items of upholstered furniture) are notoriously difficult to reproduce precisely. Since these help dictate the shape of the heat release rate curve from the overall object, and its peak, one can expect appreciable variations in measured heat release rate for such items, even with an ideal calorimeter.

4. Conclusions

The ability to reproducibly generate nominal square-wave heat release rate pulses was important to assess the transient characteristics of the large-scale HRR calorimeter without the complicating effects of the fire spread and burning of real objects. One of the key results was the determination of the minimum pulse width needed to make an accurate measurement of peak HRR. For fires with FWHH of 15 s or longer (as measured by the calorimeter), the calorimeter is capable of resolving the actual peak heat release rate value. However, if the FWHH measured by

the calorimeter was less than 11 s, the measured peak heat release rate value underestimated the actual peak heat release rate by 15% or more. The FWHH measured by the calorimeter approached a constant as the pulse width was reduced from 10 s to 5 s, indicating that the calorimeter response was controlled by flow dispersion and the time response of the oxygen analyzer.

The burner was also important to assess the repeatability performance of the calorimeter. The coefficient of variation for the repeat measurements of the peak heat release rate was typically 0.02 or less for fire pulses with a duration of 15 s or greater. Such information is important in fire tests to separate calorimeter effects from the burning characteristics of real objects.

It was found that the calorimeter was able to provide a good estimate of the total heat released for square-wave pulses changing too rapidly for the peak to be resolved by the calorimeter. That is, the integrated heat release measured by the calorimeter conserves energy to within about 5% for pulses as short as 5 s. The fast response time of the Schmidt–Boelter type radiometer was important to obtaining the most quantitative data on the gas burner output. It may be possible to combine the output of a radiometer, which has a time response of less than 1 s, with the integrated output from the calorimeter, which conserves energy, to estimate peak heat release rates for fires with FWHH as small as 3 s. The results of these experiments provide a foundation for a practical method for determining the real response time of a large-scale open calorimetry system.

References

- [1] B. Messerschmidt, P. van Hees, Influence of delay times and response times on heat release measurements, *Fire Mater.* 24 (2000) 121–130.
- [2] B. Sette, Evaluation of Uncertainty and Improvement of the Single Burning Item Test Method, Ph.D. Thesis, University of Ghent, Belgium, 2005.
- [3] R.A. Bryant, T.J. Ohlemiller, E.L. Johnsson, A. Hamins, B.S. Grove, W.F. Guthrie, A. Maranghides, G.W. Mulholland, The NIST 3 MW Quantitative Heat Release Rate Facility, NIST Special Publication 1007 (2003).
- [4] R.A. Bryant, G.W. Mulholland, A guide to characterizing heat release rate measurement uncertainty for full-scale fire tests, *Fire Mater.* 32 (2008) 121–139.
- [5] D.D. Evans, L.H. Breden, Numerical Technique to Correct Heat Release Rate Calorimetry Data for Apparatus Time Delay, NBSIR 77-1302, 1977.
- [6] A. Abramowitz, R.E. Lyon, Comparison of Heat Release Rate From Deconvoluted OSU and Oxygen Consumption Principle Calorimeter Signals, Interscience Communications Limited, London, England, 1993, pp. 161–170.
- [7] W.H. Press, B.P. Flannery, S.A. Teukolsky, W.T. Vetterling, Numerical Recipes, The Art of Scientific Computing, Cambridge University Press, Cambridge, England, 1986.